is shown in figure 5. The position of the peak and the general shape of the interference function are not altered by missing data and thus the average domain heights should be extractable even if the measured area is rather narrow. On the other hand, the attenuation is considerably higher in the curve obtained from the narrow scattering pattern. Thus the determination of the width of domain height distributions becomes wrong. Model fitting on several series of straining data from thermoplastic elastomers confirm this assessment. They show that determined distribution widths as a function of elongation can only be connected by a smooth curve, if the previous analysis of the Porod region has been performed in a sufficiently long angular interval.

References

[1] Ruland, W., (1971) *J. Appl. Cryst.* **4**, 70-74

[2] Stribeck, N., Sapoundjieva, D., Denchev, Z., Apostolov, A.A., Zachmann, H.G., Stamm, M., Fakirov, S. (1997) *Macromolecules* **30**, 1329-1339

[3] Bonart, R. (1966) *Colloid Polym. Sci.*, **211**, 14-33

[4] Ruland, W. (1977) *Colloid Polym. Sci.* **255**, 417-427

Chain Mobility in Polymer Systems; Lamellar Doubling during Annealing of Polyethylene

S.Rastogi, A.B.Spoelstra, J.G.P.Goossens and P.J.Lemstra

Eindhoven Polymer Laboratories / The Dutch Polymer Institute (DPI), Eindhoven University of Technology, Department of Chemical Engineering, P.O. Box 513, 5600 MB Eindhoven, The Netherlands.

The motion of chains in quiescent polymer melts is confined to a reptative diffusion along the contour length as proposed by De Gennes [1,2]. In the constitutive equations based on the concept of chain reptation, it is assumed that the longest relaxation times in polymer melts correspond to the reptative motion of complete chains [3]. In the case of ultra-high molecular weight polyethylene, UHMW-PE, the experimentally determined [4,5] longest relaxation times exceed 10^4 seconds.

Processing of UHMW-PE via conventional routes is virtually impossible due to the high molar mass and the excessive high melt-viscosity. The viscosity of polymer melts, above a certain threshold value for the molar mass M_c, is given by $\log \eta_0 = C + 3.4 \log M_w$, where η_0 is the zero-shear viscosity. The strong increase in the melt-viscosity with increasing molar mass is related to entanglement coupling [6] and the presence of a physical entanglement network.

Despite many efforts in the past, no advantage could be gained by processing disentangled solution-crystallised UHMW-PE via the melt. We anticipated an initial lower melt-viscosity upon heating disentangled UHMW-PE above the melting temperature in view of the fact that a certain time period is needed to form an equilibrium melt starting from (completely) disentangled systems.

Since the long chains in UHMW-PE have to reptate into each other and the tube renewal time is expected to be relatively long, in the order of a few hours [6], welding or sintering of the UHMW-PE is practically not feasible via conventional routes. In this letter, we present a summary of our recent study on enhanced chain mobility during annealing in a temperature range close to, but below the melting point of solution-crystallised UHMW-PE. The achieved chain mobility is used in welding of the two UHMW-PE films.

Characterisation techniques

By proper crystallisation from semi-dilute solutions of UHMW-PE ($M_w \sim 3 \times 10^3$ kg mol, Hoechst GUR 2122), we could make films possessing well stacked lamellar crystals. By combining small-angle X-ray scattering (SAXS), Transmission Electron Microscopy (TEM) and Low-frequency Raman spectroscopy the confined motion of the polymer chains along the chain axis has been traced.

The SAXS/WAXS studies were performed at station 8.2 of the synchrotron radiation facility available in Daresbury, U.K. [7]. A Linkam THMS 600 hot-stage mounted on the optical bench with a sample holder (capillary/film) was used to perform heating, cooling or annealing experiments. The SAXS and WAXS detectors were calibrated using the usual standards. Experimental data were normalised for the transmitted intensity and corrected for detector response and the background scattering.

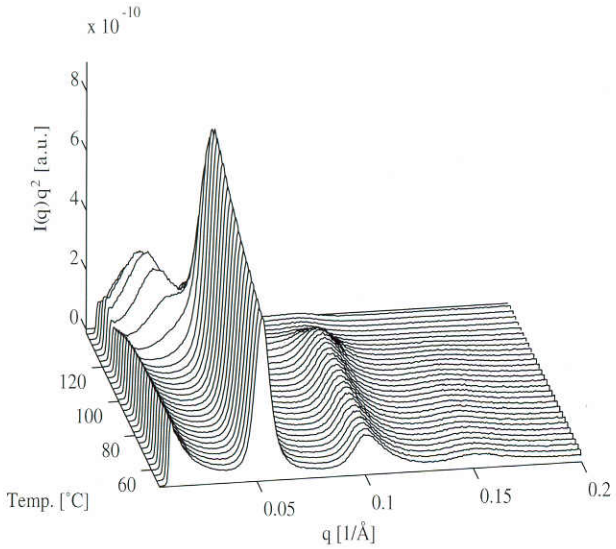

Figure 1: SAXS patterns of the solution-crystallised UHMW-PE film during a heating scan from 25 to 140°C at 10°C/min.

Raman spectra were obtained in-situ using a Dilor XY triple monochromator spectrometer. An Argon laser was used. The frequency shift of a peak with respect to the excitation line, denoted by $\Delta\nu$, expressed in cm^{-1} throughout the text, can be converted into values for the chain length within the crystalline region using the relationship derived by Schaufele and Schimanouchi [8] for paraffins. For Polyethylene, a Raman chain length, L_R, can be calculated directly from the first order by using the expression $L_R = 3169/\Delta\nu$. The morphology of the unannealed and annealed solution-crystallised films was examined using a Jeol JEM 2000FX transmission electron microscope.

Chain mobility below the melting temperature: Lamellar doubling

We have investigated the chain mobility during heating in a regularly stacked solution-crystallised UHMW-PE film. Figure 1 shows the time resolved SAXS patterns while heating at a rate of 10°C/min. At low temperatures, the SAXS patterns show three peaks with decreasing intensity along the scattering wavenumber q, satisfying the Bragg's condition for the first ($q = 0.052\,Å^{-1}$), second ($q = 0.104\,Å^{-1}$), and third ($q = 0.156Å^{-1}$) order of an average lamellar thickness of 12nm. The higher orders and sharp peaks in SAXS patterns suggest regular stacking of lamellae with nearly constant thickness. This is confirmed by TEM (figure 2a). On heating above the threshold temperature of 110°C, initially a broad weak peak at $q = 0.0262Å^{-1}$ ($d = 24$nm) appears, which becomes sharper and more intense, with diminishing intensities of the second and third orders of the 12nm crystals, and a simultaneous decrease in intensity of the first order for the 12nm crystals. The increase in lamellar thickness corresponds to a major rearrangement of chains, as confirmed by TEM in the annealed sample, figure 2b. It is evident that the thickness of the majority of the lamellar crystals increases to twice the initial value. Such a quantum increase in thickening is rather surprising and would require a proper register of lamellae with the same thickness. During heating, the loss in long range order is observed by the loss of the peaks for the second and third order. Simultaneously, the appearance of a comparatively broad peak, corresponding to a lamellar thickness of 24nm, indicates that after the quantum increase in lamellar thickness, the lamellae are no longer in perfect register as observed before heating, figure 2b. Moreover, it is intriguing to observe that after doubling, lamellae melt without substantial further thickening. Figure 3 shows a schematic representation of the increase in lamellar thickness

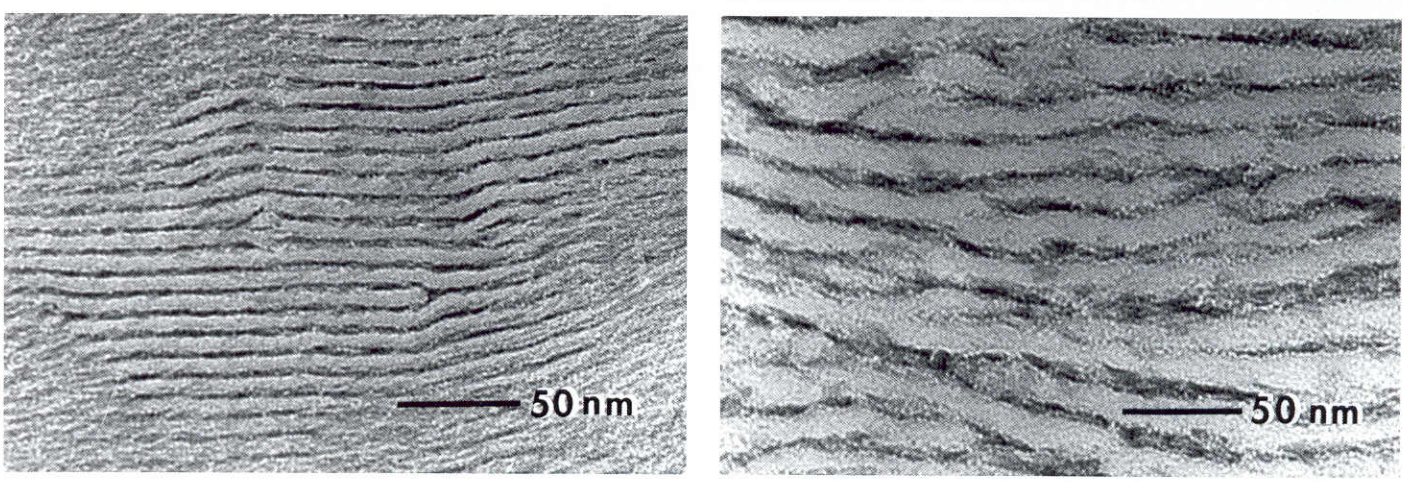

Figure 2: (Left) TEM of solution crystallised UHMW-PE film. (Right) TEM of the film annealed at 125°C for 15 minutes. Bands are lamellae as viewed edge-on.

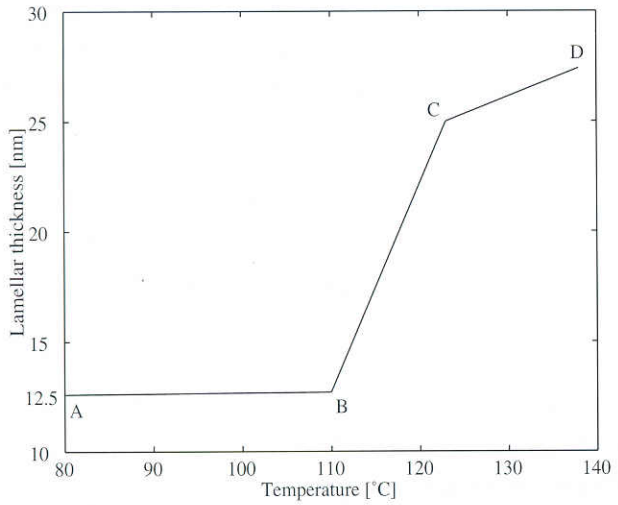

Figure 3: A schematic representation of the increase in the lamellar thickness as function of temperature.

with temperature. Lamellae start to thicken to double the initial value above point B, 110°C. Figure 3 may be divided into three different regions, AB, BC and CD. Within region AB, the lamellar thickness is constant, whereas in region BC, two different populations in terms of lamellar thicknesses, *i.e.* 12 and 24nm, co-exist. CD is the region where the logarithmic increase in lamellar thickness occurs during annealing or heating. Region BC in figure 3, which lies between 110°C to 120°C, is of significance in evaluating the mechanism involved in lamellar thickening. Therefore, it is of interest to investigate the influence of annealing within this region. A heating scan of the sample from 75°C to 115°C at the rate of 5°C/min is shown in figure 4a. Above 110°C, a few lamellae in the bulk thicken to double the initial value, while the remaining crystals do not change in terms of thickness. Thus, in the bulk of the sample two distinct populations of lamellar thickness exist. When the sample is left to anneal at 115°C, the peak intensity for the 12nm crystals decreases, while a simultaneous increase in the peak intensity for the 24nm crystals occurs (figure 4b). The rate of increase depends on the annealing temperature. When the sample is heated further beyond the annealing temperature at a rate of 1°C/min, an increase in the peak intensity for 24nm lamellar thickness occurs with the disappearance of the peak for the 12nm lamellar thickness (see figure 4c). The lamellae melt at ~135°C without substantial thickening beyond 24nm. These results clearly demonstrate that within region BC of figure 3 only two distinct populations of the crystals exist, favouring the quantized thickening in the regularly

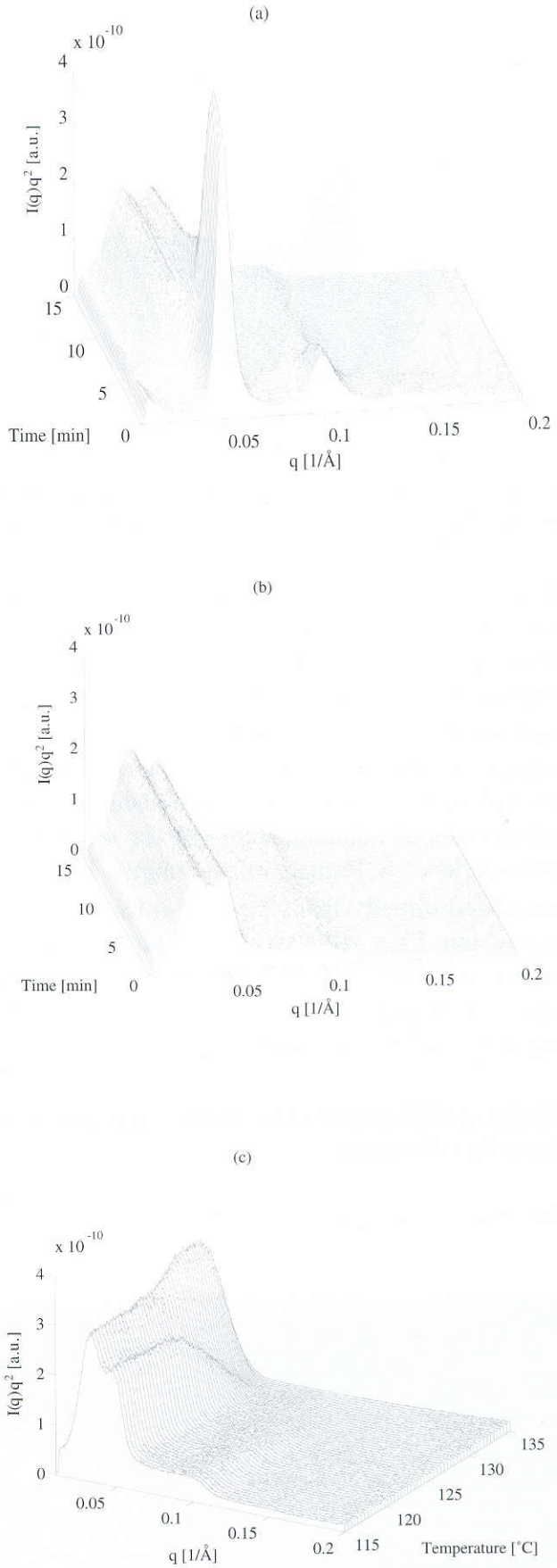

Figure 4: Time resolved SAXS patterns obtained during: (a) a heating scan from 75 to 115°C at 5°C/min (0-8 minutes) and left to anneal (8-15 minutes), (b) annealing for 15 minutes at 115°C, and (c) a heating scan from 115 to 140°C at 1°C/min.

stacked lamellae.

From the in-situ SAXS patterns alone, it is clear that the lamellar thickness increases to twice the initial value on heating, but no conclusion on the mechanism involved during thickening could be made. It may occur either via interchain diffusion between the neighbouring crystals [9] or via an increase in the amount of amorphous material in between the crystalline core [10] (*i.e.* premelting of selective small lamellae within the lamellar stacks or surface melting of the crystals) or via a melting and recrystallisation process [11]. All these mechanisms would lead to development of the SAXS pattern as observed here. To investigate the mechanism involved during chain rearrangement in the crystalline core, we performed in-situ LA Raman mode experiments at *elevated temperatures*. As stated earlier, with the help of this technique one may follow the chain motion within the crystalline core. Before application of this technique for our experimentation, it is important to investigate the influence of temperature on the LA Raman mode in general. This has been performed in detail elsewhere (Rastogi *et al* 1997, in press), a summary of the results is given below.

So far, there has not been much effort to use the LA Raman mode as a tool to reveal chain arrangement in detail at temperatures higher than room temperature. Since the SAXS pattern does not show any substantial shift after annealing the solution-crystallised film before melting, we made use of such an annealed film to investigate the shift involved in LA Raman mode due to temperature. The LA Raman peak at 13.2cm^{-1} as shown in figure 5 at 25°C, which in fact is half the value for the LA Raman peak for lamellae having a thickness of 12nm, corresponds to a lamellar thickness of 24nm. No shift in the 13.2cm^{-1} band with increase in temperature up to 135°C is observed. It may be noticed that on heating below the melting temperature the peak position does not shift, nor does the peak broaden. Close to the melting temperature, a drop in the intensity with an asymmetric broadening of the LA Raman peak towards higher frequencies occurs. The following three conclusions can be drawn from these results. First, the absence of a peak shift in the peak below the melting temperature suggests that the length of the chain segments in the crystalline core of the annealed solution-crystallised film does not vary with temperature. Secondly, the LA Raman mode in the solution-crystallised film is not influenced by the temperature. Thirdly, close to the melting temperature, 138°C, a drop in the intensity with broadening of the peak to higher frequencies (*i.e.* decrease in thickness of the crystalline core) highlights the melting behaviour of the crystalline core. The shift to lower angles in the SAXS just before the melting temperature, shown as region CD in figure 3, can therefore be associated with the melting of the crystalline core, *i.e.*, the lamellar surface, rather than interchain diffusion between the adjacent lamellae. Taking into consideration the conclusions drawn from figure 5 we will analyse our experimental observations made on the unannealed solution-crystallised film during heating as shown in figure 6 and discussed below.

Figure 6a shows a set of collected LA Raman modes at different temperatures, displayed in two dimensions. The absence of a peak shift as a function of temperature in the annealed solution-crystallised film (figure 5) indicates that the shift in the LA Raman peak in figure 6a is solely due to chain rearrangement. Figure 6a shows a sharp peak at 26.7cm^{-1} at the start of the experiment, which broadens and moves to lower frequencies above the threshold temperature of 110°C. The peak shifts gradually from 26.7cm^{-1} to 13.2cm^{-1} with increasing temperature. The maximum shift to 13.2cm^{-1} is observed at ~130°C where the peak strengthens in intensity. On cooling, from 130°C to room

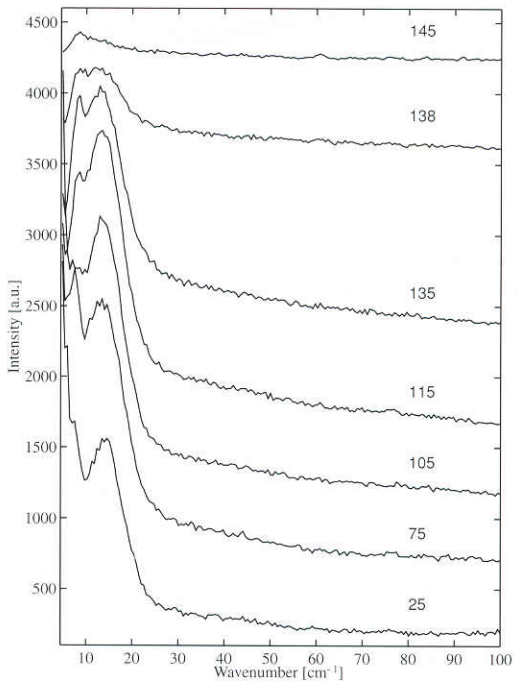

Figure 5: 2-D plot of the Longitudinal Acoustic (LA) Raman mode obtained during a heating scan from 50 to 135°C at 5°C/min of an annealed solution-crystallised film. The temperatures are indicated at the right of the figure.

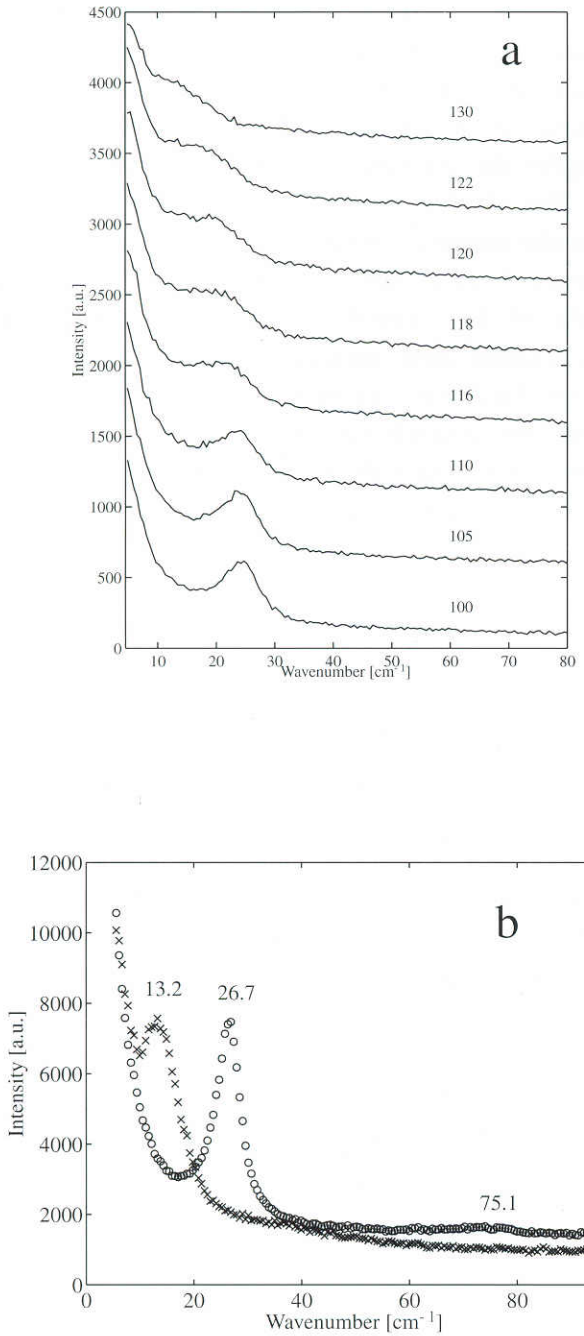

Figure 6: (a) 2-D plot of representative temperatures during heating scans (b) Comparison of the LA mode measured at room temperature between an unannealed and annealed film. (circles represent the unannealed film and crosses represent the annealed film)

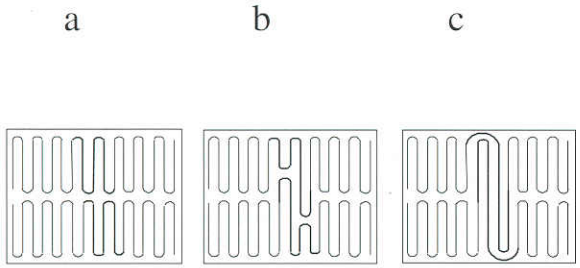

Figure 7: A schematic model to explain the doubling phenomenon in the regularly stacked adjacent lamellae. The bold line represents the test chain.

temperature, the band at 13.2cm^{-1} strengthens in intensity and becomes more distinct, as shown in figure 6b, which also shows a comparison with the unannealed film at room temperature. From the set of experiments shown in figures 5 and 6, it is clear that the crystalline core increases in thickness above the threshold temperature of 110°C to twice the initial value. The continuous shift in the LA Raman peak to lower frequencies cannot be associated with the melting of alternate lamellae or the crystalline core.

Therefore, the continuous shift in the LA Raman peak to lower frequencies clearly points to the fact that the increase in lamellar thickness is due to interchain diffusion between the regularly stacked adjacent lamellae - a situation realised in the solution -crystallised UHMW-PE films. Conversely, in the melt-crystallised polyethylene, the lamellae are arranged in spherulites and the lamellar thickness is widely distributed. Therefore the chain sliding diffusion leading to lamellar thickening cannot be realised.

The quantum increase in lamellar thickness has been observed in sharp fractionated paraffins [12], low molecular weight poly(ethylene oxide) [13,14], block copolymers (poly(ethylene oxide) and polystyrene) [15] and single crystals of nylon 6,6 [9]. The quantum increase in the thickening during the very initial stages of crystallisation in the sharp fractionated polyethylene from the melt has also been reported. One of the common morphological features, wherever the quantum increase in lamellar thickness is observed during annealing or heating below the melting temperature, is that the bulk of the material contains regularly stacked lamellae. A comparison between paraffins and UHMW-PE shows that the quantum increase in the thickening process is independent of molecular weight. This suggests that the mutual chain rearrangement between the adjacent crystals is a co-operative phenomenon where certain localised chain segments are involved, rather than the whole chain. Dislocations thus generated during thickening tend to move out of the crystal lattice to minimise the energy. A doubling scheme for the chain rearrangement between the adjacent crystals leading to doubling of the fold length has been proposed by Dreyfuss and Keller for nylon 6,6 [9] and thereafter proposed to occur by Barham and Keller [16] for the case of isothermal crystallisation of polyethylene, *i.e.*, primary thickening. With the help of neutron scattering, Sadler investigated the dimensions of

individual molecules and changes in relative positions of different molecules during the annealing of solution-grown single crystals of polyethylene. On following the chain trajectory of the deuterated molecule, it was found that on annealing at 123°C or lower the dimensions along the normal to the crystal lamellae increase in line with the lamellar thickness. During the thickening process the dimensions in the plane of crystallites were found to remain constant.

Taking the literature and our own results into account, the following model is proposed for the quantum increase in the lamellar thickness. The mechanism of the doubling process will be explained in view of the experimental details.

Figure 7a shows a schematic drawing of the regularly stacked lamellae as interpreted from the TEM of the solution-crystallised film (Figure 2a). Once the film is heated above the a-relaxation temperature, the thermodynamic driving force for lamellar thickening, necessary to minimise the surface free energy, will cause the chains to slide within the lamellae. The sliding chain within one lamella will push the chain in the adjacent lamella, as shown schematically by the bold line, representing the test chain, in figure 7b. For the sake of simplicity we have restricted ourselves to the selected region of the crystals. It has to be noted that the chains will slide between the adjacent crystals along the crystal lattice. Defects, associated with the fold surface which are introduced within the crystal lattice during chain sliding, will be removed once the crystal thickness has increased to twice the initial thickness. This is shown in figure 7c.

From figure 7c, it is evident that, once the lamellae have doubled to twice the initial value, chains get mutually entangled at the surface and further thickening via mutual chain rearrangement between the adjacent crystals can not occur. A further increase in lamellar thickness, which is logarithmic with time, should occur via melting and a recrystallisation process. In this respect our model is rather different than the one proposed by Keller and co-workers [9,16] in which thickening can occur in quantum jumps, not only giving doubling but also up to quadrupling.

Conclusions

From the above set of experiments the following conclusions could be drawn:

1. In the regularly stacked polyethylene single crystals, thickening occurs during annealing via a mutual chain rearrangement between the adjacent crystals which leads (ultimately) to a quantum increase, *i.e.*, doubling, of the lamellar thickness. The quantum increase in the lamellar thickness can be explained by our proposed model.

2. After the doubling process has been completed, further thickening via mutual chain rearrangement is hindered due to the fact that chains at the surface get entangled and, moreover, the regular stacking of lamellar crystals is lost. Further thickening of the doubled lamellar crystals involves a process of surface melting [10] or melting and recrystallisation [11].

3. The rate of increase in the lamellar thickness, ultimately leading to the quantum increase, will be dependent on the annealing temperature, *i.e.*, at higher temperatures, the doubling process will be faster.

Acknowledgement

The authors are grateful for the availability of the facilities at Station 8.2 of the Synchrotron Radiation Source (SRS), Daresbury, UK, and at Beamline ID-11/BL-2 of the European Synchrotron Radiation Facility (ESRF), Grenoble, France. Further, the authors are thankful for the experimental facilities available at Dilor, Lille, France for the Raman measurements.

References

[1] De Gennes, P.G. *Scaling Concepts in Polymer Physics*; Cornell Univ. Press, 1978.
[2] De Gennes, P.G. *J. Chem. Phys.* 1971, **55**, 572
[3] Doi, M., Edwards, S.F. *J. Chem. Faraday Trans.* 1978, **2**, 74, 1789, 1802, 1818
[4] Bastiaansen, C.W.M., Meijer, H.E.H., Lemstra, P.J. *Polymer* 1990, **31**, 1435
[5] Bastiaansen, C.W.M. *Ph.D. Thesis*; Eindhoven University of Technology, 1991.
[6] Ferry J.D. *Viscoelastic Properties of Polymers*, 2nd Ed., Wiley: New York, 1970.
[7] Bras, W., Derbyshire, G.E., Ryan, A.J., Mant, G.R., Felton, A., Lewis, R.A., Hall, C.J., Greaves, G.N. *Nucl. Instr. Meth. Phys. Rev. A* 1993, **A326**, 587
[8] Schaufele, R.F., Schimanouchi, T. *J. Chem. Phys.* 1967, **47**, 3605

[9] Dreyfuss, P., Keller, A. *J. Macromol. Sci.-Phys.* 1970, **B4**(4), 811
[10] Fischer, E.W. *Pure Applied Chem* 1972, **31**, 113
[11] Mandelkern, L. *Macromol.* 1969, **2**, 644
[12] Ungar, G., Stejny, J., Keller, A., Bidd, I., Whiting, I.C. *Science* 1985, **229**, 386
[13] Kovacs, A.J., Straupe, C. *Faraday Disc. Chem. Soc.* 1979, **68**, 225
[14] Cheng, S.Z.D., Chen, J. *J. Polym. Sci. B Polym. Phys.* 1991, **29**, 311
[15] Ryan, A.J., *et al.* Manuscript in preparation.
[16] Barham, P.J., Keller, A. *J. Polym. Sci. B Polym. Phys.* 1989, **27**, 1029
[17] Sadler, D.M. *Polymer Comm.* 1985, **26**, 204

X-PLOR for Polycrystalline Fibre Diffraction

R.C.Denny[1,2], M.Shotton[3] and V.T.Forsyth[3]

1 Biophysics Section, Blackett Laboratory, Imperial College, London SW7 2BZ
2 CLRC Daresbury Laboratory, Warrington WA4 4AD.
3 Physics Department, Keele University, Keele, Staffordshire ST5 5BG

Introduction

X-PLOR is a flexible software package for molecular dynamics, protein crystallography and NMR [1]. Among other things, the X-PLOR system allows a chosen target function to be used as an empirical X-ray energy term which can be added to the potential energy of a macromolecule. The techniques of energy minimization and simulated annealing can then be applied to the molecule to ensure reasonable stereochemistry and an optimal fit to the data. X-PLOR version 3.1 has certain limitations as far as fibre diffraction is concerned:

i) It is not possible to connect the asymmetric units of crystallographic or strict non-crystallographic symmetry together with covalent bonds.
ii) The diffraction data are treated as independent structure factors and cannot be input as composite intensities or overlapping Bessel function contributions.

A modified version of X-PLOR has addressed these problems for the case of structures with strict helical symmetry and continuous layer line intensity data and has already proved extremely useful in the study of filamentous viruses [2]. Once X-PLOR 3.1 has been installed, these new and modified routines comprising FX-PLOR can be built into the system very easily. See ***http://www.molbio.vanderbilt.edu/fibre/software.html.*** The purpose of this work is to build upon FX-PLOR to provide a system suitable for both non-crystalline and polycrystalline fibres. Two examples are given below which demonstrate the power and flexibility of FX-PLOR using simulated fibre diffraction data.

Modifications

In systems that give rise to fibre diffraction, molecules often span more than one asymmetric unit. For a molecule consisting of a simple chain of atoms this would involve defining an extra bond, two extra bond angles and three extra torsion angles to connect asymmetric units above and below the one in which the atomic coordinates of the molecule are defined. The symmetry linkage routines supplied with FX-PLOR cater for molecules where strict non-crystallographic (helical) symmetry applies. Polycrystalline fibre samples are more likely to have approximate helical symmetry and strict crystallographic symmetry. Therefore, the symmetry linkage routines in FX-PLOR required modification to allow the use of crystallographic symmetry and translations along a unit cell edge vector. This means that a continuous chain can be built passing from asymmetric unit to asymmetric unit or through the bottom and top of the unit cell.

Some of the crystallographic target functions available in X-PLOR have been adapted for polycrystalline fibre diffraction. The *F2F2* and *E2E2* target functions can be used with some modification to take account of reflection overlap. The *RESIDUAL* option has been more extensively modified to scale observed and calculated intensities together rather than structure factor moduli and to treat composite diffraction spots. These functions have been redefined for the case of a polycrystalline fibre as follows:

$$F2F2 = 1 - CC\left(\left\{w_{hkl} I^{obs}_{hkl}\right\}, \left\{w_{hkl} \sum_{h'k'l' \in M(hkl)} m_{h'k'l'} I^{cal}_{h'k'l'}\right\}\right) \quad (1)$$

$$E2E2 = 1 - CC\left(\left\{\frac{w_{hkl} I^{obs}_{hkl}}{\left\langle w_{hkl} I^{obs}_{hkl}\right\rangle_{bin}}\right\}, \left\{\frac{w_{hkl} \sum_{h'k'l' \in M(hkl)} m_{h'k'l'} I^{cal}_{h'k'l'}}{\left\langle w_{hkl} \sum_{h'k'l' \in M(hkl)} m_{h'k'l'} I^{cal}_{h'k'l'}\right\rangle_{bin}}\right\}\right) \quad (2)$$